Technological Alfvén waves

Prof. J.A. Shercliff, Ph.D., M.A., S.M.

Abstract

Though common in astrophysics, Alfvén waves have, so far, made little technological impact. The paper investigates their applicability in large homopolar energy-storage devices for use in areas such as fusion technology where up to gigawatt powers may be required for periods of the order of 1 s. Sodium is proposed for the liquid rotor. A wave device offers the attractive characteristic of delivering constant power into a resistive load, which can be matched to the characteristic impedance of the device. This impedance may be raised by the use of inductive coupling provided current reversal can be tolerated. After a discussion of ideal systems, in which dissipation is neglected, the various sources of energy loss and undesirable 3-dimensional effects (secondary flow) are investigated in order-of-magnitude terms, with reference to the relatively scanty experimental information already available. Hitherto unpublished results by Jameson concerning laboratory Alfvén waves in sodium are presented. The conclusion is that, even in the largest systems, ohmic effects on the waves cause nontrivial losses, and the advantages of an Alfvén-wave system over alternative schemes would have to be very compelling before the formidable technological task of developing large Alfvén devices could be undertaken. When the stored kinetic-energy density reaches the higher levels, secondary flow during wave transits may become a major difficulty.

1   Introduction

The Alfvén wave is the phenomenon that is most characteristic of *true* magnetohydrodynamics, where the mutual interaction of the fluid motion and the electromagnetic field is fully active, and deserves to be ranked with the other classic wave motions of physical science alongside electromagnetic and acoustic propagation. Although the Alfvén wave has several manifestations in astrophysics, it is quite remarkable how little it has figured in technology since it was first predicted by Alfvén.[1,2]

This paper is devoted to some discussion of its possible technological applications in connection with energy storage, a field which is likely to become increasingly important with the advance of fusion technology. Some proposed fusion reactor systems involve relatively slow and highly efficient cycling of very large electrical powers to and from magnet systems for confining plasma.

Flywheel/generator electromechanical energy-storage systems are well established for applications where large powers are required for times, approximately, of the order of a second, which are too long for the use of a capacitor to be satisfactory. They suffer from the disadvantage that their electrical characteristics are similar to those

Fig. 1
Homopolar flywheel/generator (Faraday disc.)

Fig. 2
Simple Alfvén wave energy store

Current flows radially in the wave between inner and outer cylindrical electrodes.

of a capacitor, i.e. as energy is extracted they slow down progressively and (unless the generator excitation is suitably adjusted) exhibit a falling voltage characteristic, just like a discharging capacitor. In practice, therefore, they are only partially 'discharged' to reduce the range of voltage variation, and most of the available kinetic energy in the flywheel is never tapped.

The idea that a pseudocapacitor, storing energy in the kinetic form, can have a liquid armature is not new (e.g. Chang and Lundgren[3]) but if the flywheel is replaced by spinning liquid metal in a cylindrical container, it then becomes possible to conceive of an armature which, instead of being *all* slowed down progressively, can have a progressive *fraction* changed in velocity by the advance of an Alfvén wave across it, the output voltage and power remaining constant: Fig. 1 and 2, respectively, show the solid and fluid-rotor schemes at their simplest. In both cases, a magnetic field B_0 is imposed, parallel to the axis. The external circuit is shown schematically. In Fig. 2 it would be constructed from axisymmetric cylindrical conductors so as to maintain the symmetry, without which the fluid motions could distort unacceptably. The Alfvén wave is, essentially, an advancing current/vortex sheet in which current (of intensity j) flows between the inner and outer electrodes, producing a magnetic $j \times B$ force which abruptly alters the azimuthal (swirl) velocity v of the fluid through which it is passing. The discharge current is, of course, associated with its own magnetic field (in the azimuthal direction) and any successful scheme must aim to liberate the energy of this field as well as the original kinetic energy of the fluid. The connections to the armature must, of course, be arranged so as not to link (and affect) the imposed field B_0.

Section 2 of this paper discusses ideal systems, in which ohmic and viscous losses are ignored, and suggests a possible improved configuration for electromechanical energy storage devices based on the Alfvén wave principle. Section 3 gives an outline of the most relevant experimental work that is available, and which has not previously been reported in the open literature (Jameson[4]). Section 4 discusses the possible complications due to ohmic, viscous and 3-dimensional effects, and attempts to identify the main areas of ignorance.

2   Ideal systems

So far, we have not discussed the details of the charging process, the liquid rotor being assumed to have been previously set into appropriate motion. If the load shown in Fig. 2 is a short circuit of low resistance, the fluid is brought to rest by the Alfvén wave (for the radially induced voltage must be zero behind it) and all the kinetic energy is progressively turned into the energy of the azimuthal magnetic field, produced by the discharge current. It can be readily verified that this is consistent with the well known properties of Alfvén waves. (see, for instance, Shercliff.[5]) The wave reflects from the right-hand end, reinstating the kinetic energy from the magnetic energy and the process repeats until ohmic and viscous effects finally dissipate the energy. No power is delivered in this case.

What is obviously required, ideally, is that the load should be a matched impedance, of such resistance that the Alfvén wave is half as strong as in the short-circuit case. On its first transit it sets up magnetic energy equal to *one quarter* of the original kinetic energy,
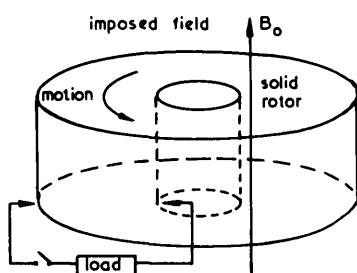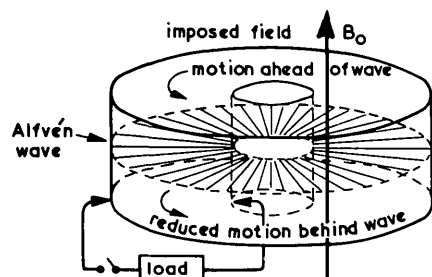
meanwhile reducing the velocity by one half, i.e. destroying *three-quarters* of the original kinetic energy, half of which is, meanwhile, delivered to the external circuit. The wave then reflects and in its return transit delivers all the remaining magnetic and kinetic energy to the external circuit, leaving the fluid at rest. No further reflection occurs, in just the same way that a matched impedance stops reflections in an electromagnetic transmission line. During discharge, the output voltage, current and power are constant.

Later we shall consider, briefly, cases where the load is not purely resistive. However, for the present we shall confine attention to the cases where the system is slowly 'charged up' from a modest power source and then fully 'discharged' into the matched load.

It is necessary to establish some feasible orders of magnitude. We shall assume that the liquid rotor is sodium, which is known to be the best electrical conductor among liquid metals, and is cheap. (The electrical conductivity $\sigma = 10^7$, approximately.) Mercury's high density might appear to make it attractive for a flywheel but it would carry the penalty that the concomitant centrifugal pressure rises would demand a very strong container. In fact, for a given strength of container, sodium could be allowed to travel faster, so as to achieve the *same* kinetic energy as the mercury. Added to which, mercury is much more expensive and unpleasantly toxic. The fire danger associated with sodium can now be regarded as covered by existing routine technology in view of the wide experience that has been accumulated with fast-fission reactors. The fact that it is a solid at ambient temperature is a positive advantage in that it then presents much less danger of leakage and fire than alternatives such as NaK eutectic, which is liquid at room temperature. It is only a minor inconvenience that a sodium system has to be heated to its melting point of about $100°C$ for operation.

The density ρ of liquid sodium at $120°C$ is 0.93×10^3 kg/m^3. This indicates that the speed of Alfvén waves, $b_o = B_o/\sqrt{(\mu_o\rho)}$, takes the approximate values:

$$b_o = 3 \text{ m/s at } B_o = 0.1 \text{ T}$$

$$b_o = 30 \text{ m/s at } B_o = 1 \text{ T}$$

$$b_o = 300 \text{ m/s at } B_o = 10 \text{ T}$$

The choice of B_o depends on the rapidity with which it is desired to extract or insert energy and whether permanent magnets or superconducting windings are to be used. If the wave is to travel 8 m, say, during discharge, $B_o = 1$ gives a discharge time of 0.27 s. $B_o = 10$ is just feasible but would be attended by difficulties in providing a controlled compact return path for the magnetic flux, whereas $B_o = 1$ would be consistent with the use of iron yokes for flux return. We shall therefore adopt the value $B_o = 1$ wherever necessary in the calculations that follow.

We assume that the complication and expense of these systems could only be contemplated in connection with large installations, such as large controlled fusion experiments or reactors where energy quantities approaching the gigajoule level might be involved. What energies can be envisaged, therefore?

Let us consider a torus of liquid sodium with a limb having a square cross-section of 4 m by 4 m and a mean radius r_m of 8 m. This choice indicates a value fairly near to unity for the ratio of the inner and outer radii. From the point of view of minimising the size of the main magnet providing B_o, the inner radius should be as small as possible but (as will be seen later) the undesirable tendency to secondary flow would then be exaggerated. This explains why a larger inner radius has been taken as the basis for discussion. The choice of a square for the cross-section is arbitrary and could be re-examined. The mass of sodium would be about 800 t. Some uncertainty attaches to the question as to what velocities in the sodium would be acceptable, and many factors might govern this choice. For the moment let us assume that centrifugal force is the dominant consideration and assert that the resulting radial pressure difference Δp must not be allowed to exceed 10^6 N/m^2 (10 atm). Actually, magnetic forces also provide a comparable radial loading on the container.

If the mean velocity of the sodium is v_m, Δp is of order $4\rho v_m^2/8$ for the torus chosen, and this equals 0.4×10^6 if $v_m = 30$ m/s, perhaps a rather high velocity for a liquid. The total kinetic energy stored would then be of the order of 0.36 GJ, which, when released in 0.27 s (two wave transits) delivers power at about 1.3 GW.

It is obvious that if the power were taken direct from the liquid rotor as in Fig. 2, it would come as a very large current at a rather low voltage. The open-circuit voltage of the system under discussion (with $v_m = 30, B = 1$) would be 120 V. Not only would the busbars have to be inordinately large (while still being fairly thin in view of the skin effect), but also the switching problems would be formidable. Some

alteration to the direct connections used in Fig. 2 is clearly necessary. Another factor to be borne in mind is the enormous dynamic load to be transmitted to the foundations if 800 t of sodium are to be stopped so rapidly.

One way of alleviating all these problems could be the following:

(a) The output voltage could be raised and the current lowered by using a multiturn secondary winding round the torus, the liquid constituting an effective primary winding.

(b) The switching process could be confined within the sodium tank itself in a way that maintained the essential axisymmetry by using an inert gas under pressure to manipulate the liquid levels between electrodes etc. (Here, the low voltages are a positive advantage in reducing the severity of gas discharges.)

(c) Two counter-rotating sodium armatures could be used to balance out the angular momentum and remove the foundation loads. This then doubles the mass of sodium, energy and power estimated above.
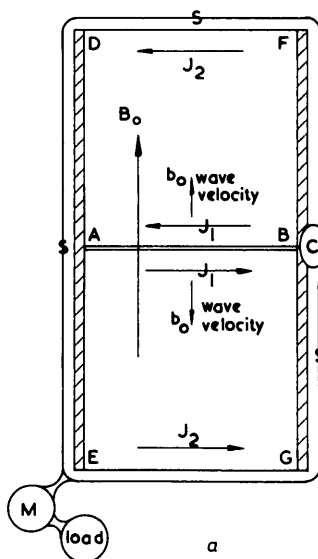

Fig. 3A
Inductive system

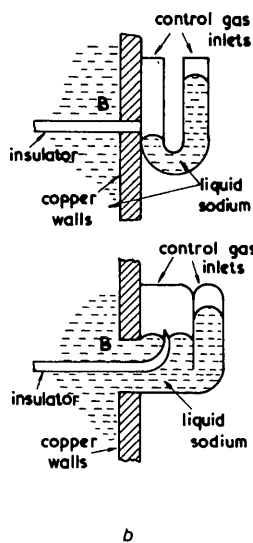Lefthand limb of torus only shown

b

Fig. 3B
Schematics of alternative contactors C

Both shown in the open-circuit state

Fig. 3A shows one of several possible schemes which embodies these principles. One counter-rotating armature is above the other, separated by an insulator AB. The outer cylindrical wall DE is a good conductor, and, in particular, allows free current flow past A between the two armatures. Direct contact between the two bodies of sodium could even be allowed here. However, the inner cylindrical conducting wall FG is interrupted at B, and C is a gas-controlled contactor that allows connection or disconnection of the two halves of FG. A schematic of possible forms for C is shown in Fig. 3B. Discharge of the

stored kinetic energy is initiated by rapid adjustment of the gas pressures in C, allowing the two bodies of sodium to make contact axisymmetrically past B, and short circuiting their combined open-circuit voltages (2 x 120 V in series). The m.h.d. of the fluid in the switch would need close examination. The resulting current sheets ($J_1 J_1$ in the figure) immediately propagate up or down the tanks as Alfvén waves. (J_1 indicates the total current in the sheet.)

The multiturn secondary windings SS round the torus, connected to the correctly matched resistive load, detects the changing azimuthal magnetic flux associated with the widening of the gap between the two current sheets, and a current I is generated in the secondary winding. The same e.m.f. induces other current sheets $J_2 J_2$ at the top and bottom, which propagate into the sodium as Alfvén waves, their current paths being completed via the highly conducting inner and outer cylindrical walls of the sodium tanks, or, alternatively, via vertical skin currents in the sodium. (Note that such current sheets do *not* propagate away from the walls, being *parallel* to the imposed magnetic field B_o.)
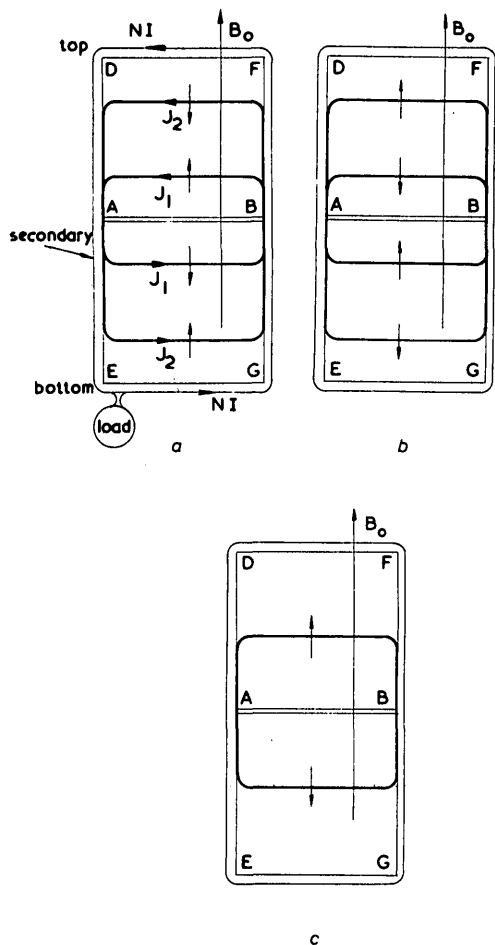

Fig. 4
Lefthand limb of torus.

The sign convention for v and azimuthal B is taken as positive *out of* the page, and this also determines the sign convention for current, as shown. The vertical arrows indicate the advance of the waves. (c) shows the state after reflection with the matched load.

The two Alfvén waves in each tank pass through each other at middepth and are reflected off the far walls simultaneously. At this instant, the voltage and current in the secondary circuit are reversed. It would be essential to have a rectifier or switch system M which could suppress this reversal, in so far as it affects the actual load, which would presumably require to draw uninterrupted d.c., and whose inherent inductance would probably not accept an abrupt reversal of current, in any case. This reversal of current is inescapable if inductively coupled systems of the type being described are to be operated in such a way that *all* the kinetic and magnetic energy is to be extracted (apart from the energy of the imposed field B_o). This is a simple consequence of the fact that the flux linked by the secondary winding is zero before and after discharge and therefore the time integral of the e.m.f. must be zero. The need to engineer M is the main drawback of the scheme under discussion.

After one reflection the waves return to the end of origin and terminate, all the energy having been extracted. The external

momentum reaction during discharge is zero. The main extra mechanical load during discharge, which has to be allowed for in the structural design, is a very large torque (about a vertical axis) transmitted between the upper and lower horizontal parts of the secondary winding. The magnet yoke could be used to carry this load. (There are no direct extra forces on the magnet system providing the imposed field B_o.) There are radial forces associated with the azimuthal (wave) field and the vertical currents in the inner and outer walls or sodium skin currents, however, which would have to be allowed for when the tanks are designed.
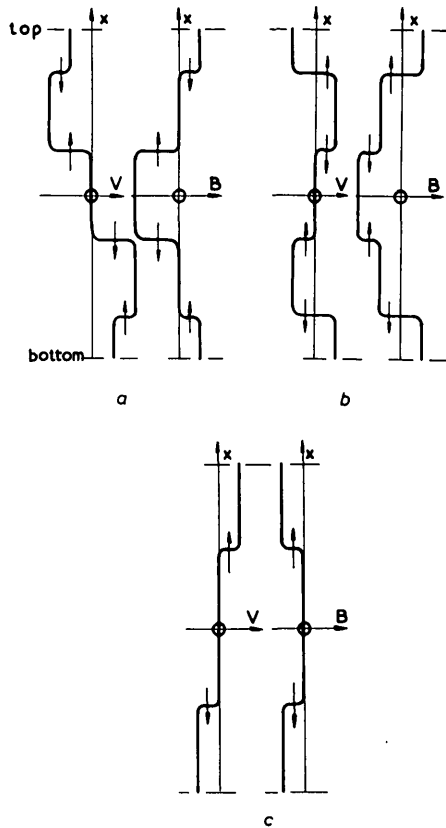

Fig. 5
Profiles of azimuthal velocity and field against depth

To justify the above assertions, let us consider the details of the waves. We shall continue to neglect viscous and ohmic losses, and to ignore secondary flow. It should be noted that the current intensity in the wave current-sheets falls off like $1/r$ (r being distance from the axis of symmetry), as does the azimuthal $j \times B$ force; and, as a result, all fluid velocities can have this same $1/r$ dependence at all stages of charging and discharging; i.e. each horizontal plane of flow is a free vortex and the only vorticity present is the radial vorticity in the waves. We shall therefore assume that this is the case and in particular that the initial velocity v_0 of the fluid has been set up in such a way that, before discharge, $v_0 = A_o/r$, A_o being a constant. The low-power charging circuit could be connected axisymmetrically across the contacting device C (in the open state) to accelerate both armatures in series. The charging time would be large compared with the wave-transit time and so the charging process would involve a rising voltage. There might be scope for varying the imposed field B_o during charging, although the associated delays (while changes of B_o diffused into the sodium), and, perhaps, fluid disturbances might be unacceptable. When charging was completed there should be no azimuthal field in the fluid.

Fig. 4 shows the state of the currents schematically at various stages during discharge and Fig. 5 shows the corresponding profiles of azimuthal velocity v and field B at a particular radius.

Let there be N turns in the secondary winding, and let the load connected in series with the secondary be a resistance Z, equal to $N^2 \mu_o b_o (\log s)/\pi$, the matched value which will be found to extract all the kinetic energy after two wave transits (s is the radius ratio of the torus). We shall assume that the secondary winding is placed so close to the sodium tanks that it links negligible flux outside the sodium.

Consider first the state shown in Fig. 4a and 5a, soon after the two sodium armatures have been connected at B, but before the inner and outer Alfvén waves have passed through each other. At any level, or value of x, the azimuthal field B, at a particular radius r from the

vertical axis, is given by Ampere's law in the form

$$2\pi r B = \mu_o \times \text{(total vertical current along FG at that level)}$$

Applying this to a level between the two upper waves (i.e. in undisturbed sodium where the field is still zero) indicates that

$$0 = NI + J_2$$

Applying it near AB, however, indicates that B_1, the field there, obeys

$$2\pi r B_1 = \mu_0 (J_1 + J_2 + NI) = \mu_0 J_1$$

while near DF the field B_2 is given by

$$2\pi r B_2 = \mu_0 NI$$

Note that in all cases B varies like $1/r$, which is consistent with having all velocities vary like $1/r$, because an Alfvén wave has the following property:

$$\frac{\text{change in transverse field}}{\text{change in transverse velocity}} = \pm \sqrt{(\mu_o \rho)} \quad \text{a constant}$$

the choice of sign depending on which way the wave is travelling (e.g. see Fig. 5a).

The value of the load resistance determines the size of I and J_2 and the strength of the waves induced at the top and bottom, because the rate of rise of flux linked by the secondary that arises from the advancing waves is equal to

$$2b_o N(\mu_o NI/2\pi + \mu_o J_1/2\pi)\log s = \mu_o b_o N(\log s)(NI + J_1)/\pi$$

in which the log term comes from a radial integration, with B varying like $1/r$. Kirchhoff's second law for the secondary circuit gives

$$-\mu_o b_o N(\log s)(NI + J_1)/\pi = I(N^2 \mu_o b_o \log s)/\pi$$

From this it follows that $J_1 = -2NI$ and $B_1 = -2B_2$ (at a given radius), which explains the wave amplitudes in Fig. 5a. Fig. 5b is amenable to a similar explanation, the waves having passed each other.

Between cases (b) and (c) reflections at the centre plane occur. Actually, these are just as if the insulator AB were absent and the waves in the upper and lower tanks merely carried on without reflection, as shown in Fig. 5c. (The insulator is only there to prevent the discharging process until the contactor C is activated.) The outer waves reach the top and bottom at the same instant as the central reflections but, with the matched load, there is no reflection at the top and bottom.

The rate of rise of flux linked by the secondary winding now becomes the negative of its previous value as the flux decays to zero again, and the current in the resistive load reverses. (See the earlier remarks about possible rectifiers or switches.) It is this reversal of current which accommodates the new boundary condition at the top and bottom, brought in by the newly arrived wave, and therefore inhibits reflection. (Note, however, that the use of any load, other than the matched resistance, would imply repeated reflections.) All action ceases when the waves in (c) complete their transit.

It is much more complicated to describe how these ideal systems behave when connected to other, possibly nonlinear, loads, e.g. highly inductive ones in a fusion confinement experiment, or perhaps even power-producing circuits in a fusion reactor with some direct conversion of the fusion energy via the plasma expansion into the confinement circuits. Other applications could be envisaged with complicated load characteristics, not describable by constant-value circuit elements such as resistors or inductors, e.g. large magnetic-forming or forging plant in which either the work-piece itself or forming tools are propelled by magnetic forces using Alfvén systems as the energy source. Large objects could, conceivably, be accelerated similarly for military or other purposes, or the energy could be dissipated suitably to release large amounts of heat or light.

Where an inductive or other linear load is used the behaviour of the direct system (Fig. 2) or the inductive system (Fig. 3) is relatively simply described until the waves reflect: it merely behaves like the open-circuit voltage in series with a resistor equal to the characteristic impedance (i.e. the same value as the matched load resistor). This is easily demonstrated from the wave equations. The behaviour after reflections, however, becomes rather complicated.

The question also arises as to whether these Alfvén-wave devices are attractive as energy stores in oscillatory systems, where energy moves periodically between a store and the main device, which might be an inductive magnet system for a cyclic form of fusion reactor. If energy losses are ignored, it is a simple matter to examine the steady modes of oscillation that are possible with, for instance, a pure inductance L connected to the Alfvén system shown in Fig. 3,

with the contactor C closed or the insulator AB omitted. We are now describing something very close to the standing-wave experiments of Jameson,[6] who used a multiturn secondary winding to induce oscillatory Alfvén-wave modes in a torus of sodium. Let the total depth of the tanks be $2l$.

The standing wave modes will be describable by the equations

$$v = (A/r) \sin kx \cos kb_o t \quad \text{(A is constant)}$$

and

$$B = \sqrt{(\mu_o \rho)}(A/r) \cos kx \sin kb_o t$$

which obey the m.h.d. equations (with describable by the equations effects ignored):

$$B_o \frac{\partial v}{\partial x} = \frac{\partial B}{\partial t} \quad \text{and} \quad \rho_o \frac{\partial v}{\partial t} = \frac{B_o}{\mu_o} \frac{\partial B}{\partial x}$$

The magnetic flux linked by the secondary is

$$N\{\sqrt{(\mu_o \rho)}\}(A \log s)\sin kb_o t \int_{-l}^{l} \cos kx\, dx =$$

$$\frac{2N\{\sqrt{(\mu_o \rho)}\}(A \log s)\sin kb_o t \sin kl}{k}$$

The value of B at $x = \pm l$, namely $\{\sqrt{(\mu_o \rho)}\}(A/r)\cos kl \sin kb_o t$, must be compatible with the secondary ampere turns NI, for

$$2\pi r B = \mu_o NI$$

Hence, $2\pi A\{\sqrt{(\mu_o \rho)}\} \cos kl \sin kb_o t = \mu_o NI$ and the flux linked by the inductance is LI. In the oscillating mode, the total flux linked by the secondary circuit (resistance being negligible) is zero, and it follows that

$$\tan kl + Rkl = 0,$$

in which

$$R = \frac{\pi L}{\mu_o N^2 l \log s} = \frac{L/Z}{l/b_o}$$

the dimensionless ratio of two characteristic times. The first root for kl lies between $\pi/2$ and π, and the corresponding v and B profiles are shown in Fig. 6. The corresponding angular frequency is kb_o.
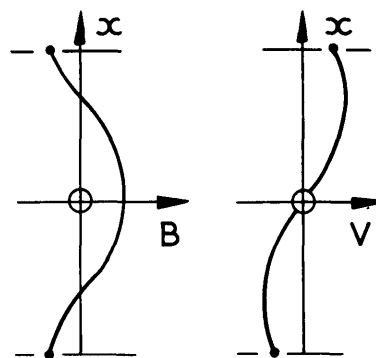

Fig. 6

Profiles of azimuthal velocity and field (oscillatory case, inductive load)

The Alfvén device is now acting like a capacitor and, in fact, is not now doing anything that a solid-rotor energy store could not offer, although it might have detail advantages for certain applications, e.g. the absence of moving parts and brushes etc. It suffers from an inefficiency in that, although the energy in the inductor periodically falls to zero, the total energy in the Alfvén device does not. This is in contrast to the case where it is discharged into a matched resistive load. The maximum and minimum stored energies are in the ratio

$$\frac{1 + R\cos^2 kl}{1 - R\cos^2 kl}$$

A further question concerns the scope for manipulating the energy transfers between an Alfvén device and its load to achieve a desired programme of events (e.g. stages of plasma compression in a fusion reactor). The most obvious stratagem, apart from opening and closing the contactor C, would have been to program the strength of the field B_o, on which the Alfvén waves ride, had it not been the case that the long diffusion times for fields into sodium preclude this. The idea of *propagating* (rather than diffusing) changes of the

imposed field into the sodium by means of secondary Alfvén waves (riding on a weak auxiliary field in another direction) is ruled out by the fact that such Alfvén waves would involve velocities in directions that are incompatible with the walls of the container as at present conceived. It is not inconceivable that a very much more subtle field/container geometry could be arrived at which allowed 'control' Alfvén waves to alter the speed of the main Alfvén waves, however.

The only other stratagems for manipulating the energy flows would be altering the turns ratio by tap changing (a formidable prospect at the gigawatt level) or by dissipation of energy in resistors in the primary (contactor) or secondary circuits, which would probably be wholly unacceptable in the fusion-reactor context, where energy conservation is of the essence, the circulating magnet powers being so large. In fact, because of the viscous and ohmic dissipations, some power *supply* must be inserted at appropriate stages either in the secondary or primary (contactor) circuits. This, in itself, offers some further control stratagems.

It is clear that a great deal of systems-design work would have to be done before an Alfvén device could be optimised and appraised for each potential application.
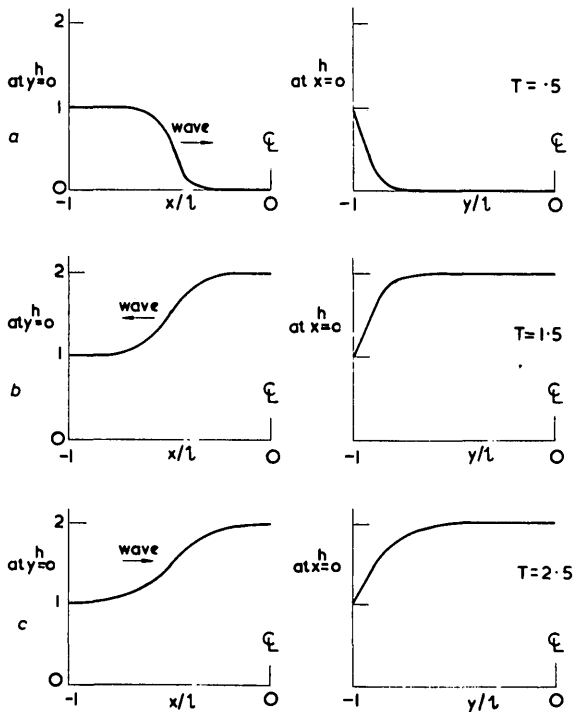

Fig. 7

Magnetic field profiles at successive instants (Λ = 0·01)

h = field as a fraction of its surface value established by the input step current in the secondary
T = time as a fraction of the half-transit time l/b
(b) refers to a state after the two waves have passed through each other and
(c) shows a wave after one reflection.
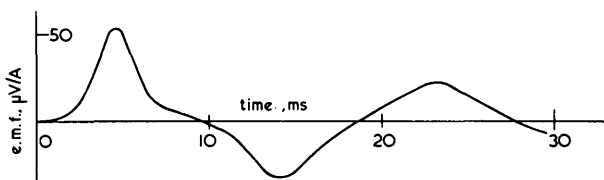The transverse profiles at x = 0 are on the right

Fig. 8

Predicted induced e.m.f. per unit input current for small search coil

Effective Λ = 0·0495

3   Jameson's work

Jameson performed experiments in which Alfvén waves were produced in sodium, in a torus having inner and outer radii of 38 mm and 275 mm respectively, and sodium depth $2l = 175$ mm, by a secondary exciting winding of 20 turns carrying currents of the order of 20 A. The imposed vertical field took values up to 0·65 T. The existence of the waves was demonstrated by a search coil with 10 turns of 19 mm diameter, located so as to detect azimuthal fields at

the centre of the sodium, and also by a large search coil mounted round the limb of the torus. Jameson's waves were small-amplitude waves in which nonlinear 3-dimensional effects due to centrifugal forces etc., would be quite negligible. He compared theoretical predictions of the behaviour, allowing for viscous and ohmic dissipation (including that in the thin-walled (1·2 mm) stainless-steel sodium tank) with his observed results. Jameson's paper[6] describes his apparatus and presents the theory and results for experiments in which standing waves were produced by employing a sinusoidal input to the secondary winding. Convincing resonances were demonstrated, and the theory and observed amplitudes and frequencies were in good agreement.
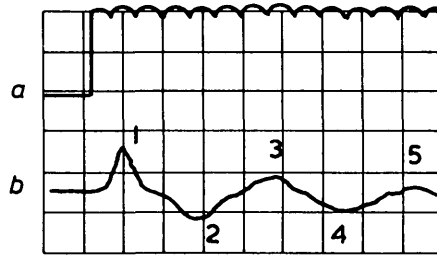

Fig.9

Experimental results from the small search coil

(a) Input current (scale: 10·4 A/div)
(b) Induced e.m.f. (scale: 1 mV/div)
Time scale = 5 ms/div

Jameson reported other equally successful experiments on progressive waves in his thesis.[4] In these experiments input was a step wave of current, which excited diffusing Alfvén step waves at the top and bottom of the sodium. The waves should reflect back and forth before finally decaying. We reproduce here some of Jameson's figures. Fig. 7 and 8 show theoretically predicted results, while Fig. 9 is taken from the observed oscilloscope traces.

Jameson used the parameter Λ, which equals $\lambda/b_o l$, λ being the magnetic diffusivity $1/\mu_o \sigma$. Λ is an inverted Lundquist number and needs to be small to allow good Alfvén waves which make many transits before being damped. (In one half transit, lasting a time l/b_o, a step-wave diffuses to a width of the order of $\sqrt{(\lambda l/b_o)}$, which is small compared with l if Λ is small.) Jameson's calculations were carried out for Λ = 0·1 and 0·01, with viscous effects ignored. He took a square section for the torus and the mean radius of the torus was so large that curvature effects could be ignored. The walls were assumed to be nonconducting. The method involved a double Fourier series.

Fig. 7 shows the calculated field profile against x (the arrows indicating the advancing wave) and against y on the centre plane x = 0, y being the radial distance measured from the centre of the square section. The x profiles show the broadening of the wave due to ohmic dissipation and the y profiles show the very similar diffusing of the current 'sheets' on the walls parallel to the imposed field. (This effect is reduced if these walls are highly conducting.) Jameson describes the effect as 'transverse degeneration towards sine-wave form'. Fig. 7 is drawn for the case Λ = 0·01.

Fig. 8 shows the predicted signals in the search coil in the centre of the sodium at the highest imposed field (0·65 T) used by Jameson. The ordinate is the e.m.f. per unit of input step current in the secondary. In calculating these values, Jameson made some allowance for the small effects of viscosity, which increased the effective value of Λ to 0·0495 for the case shown in Fig. 8. No allowance was made for the finite size of the search coil as the wavefront was already much broader than the coil even on its first encounter with the coil. It will be noticed that the figure shows three transits of the wave, by which time successive waves are intermingling.Fig. 8 shows results calculated for the actual dimensions of the experimental torus, which was not square in section.

Fig. 9 is the corresponding experimental result, a tracing of a cathode ray oscilloscope record. The upper trace shows the exciting step current. Its ripple would have only minor effects deep in the sodium, although Jameson found that it confused the signals detected by his other *large* search coil (round the limb of the torus). The lower trace shows the actual signals in the search coil for five transits of the waves (numbered in the figure). The close resemblance of 1, 2 and 3 to Fig. 8 is apparent, and the quantitative agreement is also satisfactory.

For fields of 0·487 T, three transits could be clearly detected but as the field fell to 0·325 T (Λ = 0·1) the waves were becoming rather diffuse and not easily distinguished. Nevertheless, Jameson's results

clearly demonstrated not only the existence of progressive Alfvén waves in liquid metals, but also the efficacy of energy exchange between a liquid armature and a secondary winding by induction*.

The work of Jackson et al[7]. at MIT should also be noted. He successfully demonstrated Alfvén waves in a system of the type shown in Fig. 2, using NaK eutectic. The depth of the torus was comparable to that of Jameson but the radii were smaller. The apparatus and results are also included in the authors' filmt on magneto hydro-dynamics.

4 Dissipative and 3-dimensional effects

In this Section some important effects are examined which have been largely ignored so far but which would need close investigation before Alfvén devices could be seriously contemplated.

For the large system discussed in Section 2, with $B_o = 1$ T and $2l = 4$ m, say, the parameter Λ equals 0·0014 approximately. This small value means that a step wave broadens to a thickness of order $\sqrt{(\Lambda)}l$ or 0·37l on travelling a distance l. Though the actual kinetic energy and magnetic energy lost is small, the reflection processes now lose their ideal instantaneous quality.

More serious are the energy losses associated with the diffusion of the current sheets into boundary layers at the walls parallel to the imposed field, as evidenced on the right of Fig. 7. The losses may be partly dissipation and partly failure to extract all the kinetic energy because the current loops do not go right across the channel. If these layers are not alleviated by having highly conducting walls in parallel, or if contact resistance proves to be a problem, these layers also grow to a thickness of the order of $\sqrt{(\Lambda)}l$ while the wave travels a distance l. This means that a fraction of the order of $\sqrt{(\Lambda)}$ of the volume of the torus exchanges kinetic/magnetic energy significantly below the ideal values, and these energy losses, of the order of 3 to 4%, might be regarded as unacceptable, not least because of the large amount of cooling that would be involved. It would appear that highly conducting side walls would be essential. Copper has a conductivity that is about 5 times better than sodium and could therefore offer considerable relief if thick enough (i.e. at least as thick as the relevant skin thickness). The ability of suitably supported copper to withstand prolonged exposure to liquid sodium as well as the high centrifugal and magnetic pressures would need confirmation. Serious engineering problems might arise over the making of satisfactory joints between the highly conducting vertical walls and the insulating, or at least weakly conducting, horizontal walls. The rapidly fluctuating pressure loads would tax the joints and structure severely.

Viscous effects become important in schemes where the motion of the fluid in other than wave modes is of interest, e.g. where the system is slowly 'charged' in a nonwave manner before a rapid discharge into a matched load. There the question of the losses in a more or less steady state of rotation becomes important. Let the viscosity be η (6·3 × 10^{-4} for sodium at 120° C).

In a straight nonconducting channel of rectangular cross-section, with no pressure gradient, an initial state of uniform axial velocity decays under the influence of boundary layers of constant thickness, the core velocity staying uniform in space. The process is relatively slow and the Alfvén mechanism is inactive. If turbulence is absent. the dominant phenomenon is the Hartmann layer,[8] to be found on the walls normal to the imposed field (see Fig. 10). These viscous layers of slower fluid, in which the horizontal $v \times B$ e.m.f. is deficient, provide a constricted return path for the currents which can circulate, as shown in the figure. The thickness of the layers is l/M, where M is the Hartmann number $B_o l \sqrt{(\sigma/\eta)}$. The current loops are completed via boundary layers of thickness of order $l/\sqrt{M}$ on the vertical walls or via these walls, if conducting. For the systems discussed in Sections 2 with $B = 1$ and $l = 2, M$ would be of the order of 250 000, which is a very high value and far beyond present experimental experience. Obviously, any significant conductivity of the horizontal walls could provide a much readier return path than the Hartmann layers and should therefore be avoided. With non-conducting horizontal walls, the circulating current in the Hartmann layers per unit streamwise length is $v\sqrt{(\sigma\eta)}$, in which v is the uniform velocity in the central core of the flow. The current density in the core is therefore $v\{\sqrt{(\sigma\eta)}\}/l$ and the magnetic-drag-force density is $Bv\{\sqrt{(\sigma\eta)}\}/l$, equal to $-\rho dv/dt$ as the fluid slows down. The fluid decelerates exponentially with a time constant equal to $\rho l/B\sqrt{(\sigma\eta)}$, which for the schemes of Section 2 is of the order of 23 s. Evidently, if charging or waiting times approach or exceed this relatively low value, significant energy losses will be encountered. It is not obvious that there is any easy remedy for this loss due to the Hartmann

layers other than lowering the value of B, unless it were possible to devise new topologies in which the imposed field never has a component normal to a wall. The one advantage that mercury offers over sodium is that the decay times are 28 times longer. Perhaps short streamwise insulating fins could be used to break up the Hartmann layers. Heiser and Shercliff[9] reported experiments in mercury in toroidal geometry which included decelerating flows, albeit with the imposed magnetic field radial rather than axial. In the schemes of Section 2, with an axial field, the velocity would retain its $1/r$ dependence while slowing down, provided that secondary flow was negligible.
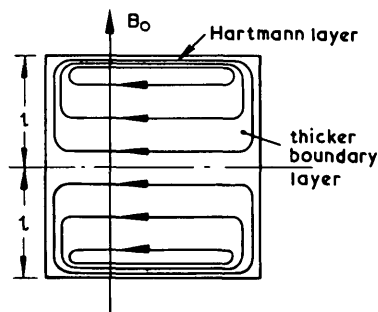

Fig. 10
Currents circulating through Hartmann layers

A further question is whether viscous laminar flow would prevail. The thicker boundary layers on the vertical walls would probably become turbulent first but would have relatively little influence. Only limited experimental data are available, all taken at values of M below 1000, and therefore somewhat questionable if extrapolated to an M of 250 000. Murgatroyd[10] indicated that turbulence in Hartmann flow between planes was suppressed for $R/M < 225$ while in the schemes of Section 2, with $v = 30$ m/s, the Reynolds number $R = \rho v l/\eta = 9·10^7$, approximately, and R/M is about 350, which suggests that somewhat lower velocities might be necessary to avoid turbulent Hartmann layers (which would then be thicker and allow bigger eddy currents). Further tests at higher values of R and M would clearly be desirable to confirm this conclusion, although once M is large, the two Hartmann layers behave more or less independently and their stability should depend only on R/M, which is the Reynolds number based on Hartmann-layer thickness. Turbulence, even in the other boundary layers, might also be unacceptable because of noise, possible fatigue danger in the container, or perhaps cavitation damage in regions of low pressure and high velocity near the inner wall of a toroidal system.

One surmises that turbulence and other instabilities do not constitute a problem in connection with wave-like modes of behaviour. However, it is not absolutely clear whether, over a series of events, with constantly growing boundary layers on the vertical walls, the fluid motions in a toroidal system might stray so far from the $1/r$ dependence of the ideal state that wholly undesirable, perhaps nonaxisymmetric motions might set in. This area of stability theory is almost wholly unexplored. Baylis[11] reported experiments on Taylor-type instabilities observed in magnetically driven circular flows between long concentric stationary conducting cylinders in the presence of an axial magnetic field and radial current flow and compared them with theory by Chandrasekhar. They have little bearing on the present cases which are dominated by the top and bottom walls, however.

Mention of Taylor instabilities leads us to our final topic, the possible influence of other 3-dimensional effects associated with centrifugal and coriolis forces and analogous magnetic forces. Consider, for instance, the toroidal system shown in Fig. 2. Obviously, the centrifugal forces will be different ahead of and behind the Alfvén wave and one would expect to see streamwise vorticity, i.e. secondary flow, appearing.

When waves are travelling in *one* direction only and dissipative effects are unimportant, the tendency to secondary flow can, under some circumstances, be suppressed by the magnetic forces associated with the magnetic field of the waves. This is easily seen if we adopt the approach of Walén.[12,13] By using axes moving with the wave so as to achieve steady flow, we can satisfy the equations of ideal, steady m.h.d., namely,

$$\rho(v \, \text{grad})v + \text{grad}(p + B^2/2\mu_o) = (B \, \text{grad})B/\mu_o$$

and

$$\text{curl } v \times B = 0,$$

by taking $B = \sqrt{(\mu_o\rho)}v, p + B^2/2\mu_o$ being constant. A particular case is a unidirectional axisymmetric Alfvén plane wave of the type discussed in Section 2, reduced to rest by having an axially moving frame of reference. The condition $B = \sqrt{(\mu_o\rho)}v$ implies that it is a wave in which the azimuthal field and velocity are in the constant ratio $\sqrt{(\mu_o\rho)}$. In particular, such a wave has zero azimuthal field where it has zero swirl, as for instance initially in Jameson's experiments where the wave is launched into fluid at rest devoid of azimuthal field. In such a case there is no tendency to secondary flow; the centrifugal pressure variations are exactly compensated by the variations of the axial $j \times B$ forces in the wave front. However, the case shown in Fig. 2, where moving fluid having no azimuthal field is brought to rest by the wave, cannot be reduced to a Walén flow by a moving frame of reference and is therefore prone to secondary flow. In fact, here the centrifugal forces and the axial $j \times B$ forces in the wave co-operate in promoting it. Furthermore, in general, there are waves travelling in both directions and no possibility of reduction to a Walén flow exists.

No study of these nonlinear secondary effects in axisymmetric Alfvén wave systems appears to have been attempted. Here, we shall confine ourselves to order-of-magnitude ideas.

Consider the simple case shown in Figs. 2 and 11, at the instant when the wave is halfway across, the fluid ahead having a swirl velocity v, proportional to $1/r$, the fluid behind having half this speed. In the Alfvén wave LM, $j \times B$ produces an upward force with magnitude per unit area of wave equal to $B^2/2\mu_o$ (B being the azimuthal field). This equals $\rho v^2/8$ in view of the jump condition
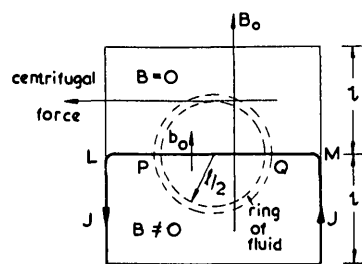

Fig. 11
The generation of secondary flow

$\Delta v = \Delta B/\sqrt{(\mu_o\rho)}$ across Alfvén waves. The ring of fluid of radius $l/2$, say, and cross-section ϵ, shown in Fig. 11, is subjected to a magnetic torque and a centrifugal torque about its centre C. (n.b. It is not suggested that the secondary streamlines would be exact circles.) The magnetic torque is due to the difference in $\rho v^2/8$ at P and Q, associated with the radial velocity variation. This difference is approximately $\rho v_m^2 l/4 r_m$, v_m being the mean velocity and r_m the mean radius. The resulting torque is $\epsilon\rho v_m^2 l^2/8r_m$. Integration round the ring shows that the centrifugal torque is approximately $\rho\epsilon v_m^2 l^2/2r_m$ (from the fluid above LM) less a counter torque $\rho\epsilon v_m^2 l^2/8r_m$ (from the fluid below LM). The combined torque is approximately $\rho\epsilon v_m^2 l^2/2r_m$ which gives the fluid ring a peripheral acceleration a whose magnitude is given by

$$\rho\epsilon v_m^2 l^2/2r_m \approx \rho\pi l^2 \epsilon a/2 \quad \text{i.e.} \quad a \approx v_m^2/\pi r_m$$

This estimate of a crudely represents the growth of secondary velocities, which might be expected to be most rapid when the wave is at half transit. The secondary velocities rise to roughly al/b_o in one wave transit, if we take the average acceleration as $\frac{1}{2}a$. Secondary flow will be unimportant if these velocities, of the order $lv_m^2/\pi b_o r_m$, are small compared with the Alfvén speed b_o, so that the waves continue to travel through virtually stationary fluid. We therefore need the ratio $L = lv_m^2/\pi b_o^2 r_m$ to be small. Note, however, that the radial motion would tend to convect the imposed field radially inwards or outwards and the resulting Maxwell stresses would therefore inhibit the secondary displacements to some extent. We may therefore be overestimating the secondary flow, but the distortion of the imposed field might be equally deleterious. A more exact analysis of the process would have to study the detail creation of vorticity which occurs at the wavefront.

For the case discussed in Section 2, with $b_o = v_m = 30$ m/s, $l = 2$ and $r_m = 8$, the ratio L is about 0·08 and secondary flow appears to present a fairly serious problem. One way of alleviating this is to make the torus of larger diameter so that the ratio of the inner and outer radii can be nearer unity and the flow more closely approximates to that in a straight duct, where secondary flow is absent. Another way might be to change the geometry so that the

Alfvén waves are radially travelling cylinders, the imposed field being radial (and nonuniform, so that the Alfvén speed varies) and the current axial. The only secondary flow would then be that associated with the nonuniform magnetic and centrifugal forces in the boundary layers on the plane top and bottom walls, parallel to the imposed field.

Sometimes the sign of the secondary flow generated by successive transits of the wave after reflection reverses and then there would be some corrective action, but this does not always occur.

For schemes which involve significant periods of quasisteady flow, without waves present, another source of secondary flow occurs, namely the reduced centrifugal force in the Hartmann layers. During slow charging or a waiting period, a quasisteady state of primary flow round the torus, modified by secondary flow, can be established. Such situations were also studied by Baylis,[14] who performed experiments on steady mercury flows in toruses of square cross-section and various radius ratios, with an axial magnetic field and an imposed radial driving current between the highly conducting cylindrical electrode/ walls, the plane walls being insulators. The square cross-section has side $2l$ (or d in Reference 14).

The parameter which controls steady secondary flow in curved ducts, in the absence of magnetic effects, is the Dean number k, given by

$$k = R\cdot\sqrt{(d/r_m)}$$

in which d is a dimension of the cross-section, r_m is the mean radius of curvature of the duct and R is the Reynolds number (based on d). At high k there are boundary layers (in which the centrifuged flow returns towards the axis) of thickness of the order of $d/\sqrt{k}$.

Baylis points out that adding m.h.d. effects produces the following four regimes:

(a) $M^2 \gg k$, in which secondary flow is suppressed and the motion resembles Hartmann flow in a straight channel
(b) $M^2 \approx k$, a complex transitional regime
(c) $M^2 \ll k$, in which magnetic effects are weak and ordinary 'Dean' flow, dominated by secondary flow, occurs
(d) when k is large enough, a turbulent regime.

From values of M around 16 up to 130, which was Baylis's highest value, the transition from regime (a) to (b) took place near $k/M^2 = 1$.

If we risk extrapolating Baylis's results to the much higher values of M which prevail in the schemes of Section 2, we find that $k = 1·27 \times 10^8$ whereas $M^2 = 6·3 \times 10^{10}$ if $B = 1$ T. Under such circumstances, Baylis-type secondary flow would be negligible but this might not be the case if lower fields or higher velocities were used. It does, nevertheless, appear that secondary flow during the wave phases of operation is the more serious problem.

5   Concluding remarks

It is apparent that the rewards offered by Alfvén energy stores (their potentially large power outputs and constant-power characteristics when loaded resistively) would not be easily won. Considerable expense and the development of untried technology would be involved, but in the context of activities like fusion technology such a situation is normal. Obviously, the necessary effort for developing Alfvén devices would not be forthcoming unless more traditional systems were incapable of meeting the demands of the situation or could be undercut by an Alfvén device, even after allowing for its high development costs.

It is clear that in any application where good electrical energy conservation (as between charging and discharging) is essential, only the largest devices can be contemplated, because of the energy losses associated particularly with the side boundary layers in imperfectly conducting liquids. There appears to be no prospect whatever of finding a better conductor than sodium. And even in the largest devices energy losses of the order of 4% per wave transit appear likely unless conducting walls can provide relief. The losses appear as low-grade heat which is not reclaimable for steam-rising purposes as the liquid sodium must be kept as cool as possible to maintain its conductivity. The Hartmann losses during slow charging or waiting periods may also pose a severe problem.

Before any serious design work could be attempted it would be necessary to perform experiments or computer investigations to establish how seriously the wave action is disrupted by secondary flow at various velocity levels, and whether the fluid armature behaves acceptably through a long series of repeated charge and discharge events in the face of the imperfections due to finite conductivity. One would be fairly confident that the imposed field B_o would tend to quell most 3-dimensional aberrations, although it has little effect on vorticity parallel to itself, associated for example

with velocity distributions not proportional to $1/r$, except via the dominant influence of the Hartmann layers upon all fluid lying along the same field line. (See for instance Hunt and Shercliff.[8]) This has the effect of maintaining the state $v \propto 1/r$ more or less indefinitely during and after slow-speed charging.

It is not suggested that the configurations discussed in Section 2 are the only, or even the best, designs. They are chosen because sufficient information is already available to allow reasonable understanding of their likely behaviour. They suffer from the inevitable disadvantage of current reversal, necessitating switches or rectifiers at the half-discharged point, as the penalty for using inductive coupling as a way of raising the apparent characteristic impedance of the wave system. There may well be more subtle possibilities in which, for instance, most of the energy of the imposed field on which the waves ride is also able to be discharged, leaving the fluid field free and stationary.

6   References

1 ALFVÉN, H.: 'On the existence of electromagnetic-hydromagnetic waves', *Ark. Mat.*, 1942, **29B**, (2)
2 ALFVÉN, H.: 'Existence of electromagnetic-hydrodynamic waves', *Nature*, 1942, **150**, pp. 405–6
3 CHANG, C.C. and LUNDGREN, T.S.: 'Flow of an incompressible fluid in a hydromagnetic capacitor', *Phys. Fluids*, 1959, **2**, pp. 627–632
4 JAMESON, A.: 'Magnetohydrodynamic waves', Ph.D. thesis, Cambridge University, 1961
5 SHERCLIFF, J.A.: 'A textbook of magnetohydrodynamics' (Pergamon, 1965)
6 JAMESON, A.: 'A demonstration of Alfvén waves; the generation of standing waves', *J.Fluid.Mech.*, 1964, **19**, pp. 513–527
7 JACKSON, W.D., GOTHARD, N., and CARSON, J.F.: *Bull. Am. Phys. Soc.*, 1964, **9**, Section II, p. 587
8 HUNT, J.C.R., and SHERCLIFF, J.A.: 'Magnetohydrodynamics at high Hartmann number', *Ann. Rev. Fluid Mech.*, 1971, **3**, pp. 37–62
9 HEISER, W.H., and SHERCLIFF, J.A.: 'A simple demonstration of the Hartmann layer', *J. Fluid Mech.*, 1965, **22**, pp. 701–707
10 MURGATROYD, W.: 'Experiments on magnetohydrodynamic channel flow', *Philos. Mag.*, 1953, **44**, pp. 1348–1354
11 BAYLIS, J.A.: 'Detection of the onset of instability in a cylindrical magnetohydrodynamic flow', *Nature*, 1964, **204**, p. 563
12 WALÉN, C.: 'On the theory of sunspots', *Arkiv. Mat.*, 1944, **30A**, (15)
13 WALÉN, C.: 'On the distribution of the solar general magnetic field', *ibid.*, 1946, **33A**, (18)
14 BAYLIS, J.A.: 'Experiments on laminar flow in curved channels of square section', *J. Fluid Mech.*, 1971, **48**, pp. 417–422

IEE Conference Publication 142

Advances in magnetic materials and their applications
(1st–3rd September 1976, Savoy Place, London)

The following contributions appear in IEE Conference Publication 117:

ABEL, E., MAHTANI, J.L., MULHALL, B.E., and RHODES, R.G.: An assessment of linear superconducting motors for Maglev

ADAM, J.D., and DUNSMORE, M.R.B.: Low-loss microwave filters using epitaxial yttrium iron garnet

ALBRECHT, C.: Development of levitated vehicles with superconducting magnets

ANDRES, U.Ts., LIN, I.J., and YANIV, I.: Magnetic susceptibility and viscosity of paramegnetic solutions for m.h.s. separation of solid particles

APPLETON, A.D., and DOBBING, P.P.: A discussion on some aspects of high-gradient magnetic separation

BACHMANN, K.: Rare-earth-cobalt permanent magnets

BASAK, A., and MOSES, A.J.: Effects of normal flux on power loss in grain-orientated silicon-iron laminations

BASZYNSKI, J.: Monocrystalline, epitaxial growth of ferrite layers from the vapour by chemical transport

BINNS, K.J.: Future uses of permanent-magnet materials in electrical machines

BIRSS, R.R., GERBER, R., and PARKER, M.R.: Analysis of matrix systems in high-intensity magnetic separation

BOHN, G.H.: The influence of eddy currents on an electromagnetic levitation system

BURNETT, J., and OVERSHOTT, K.J.: Analysis of the dynamic operation of permanent magnets

CAMPBELL, P., and JOHNSON, R.B.I.: Forces on magnetically levitated vehicles above flat guideways: a modelling technique

CARPENTER, C.J., and LOWTHER, D.A.: Losses due to transverse fluxes in laminated iron cores

CHAMBERLAYNE, J.W., and GILES, A.D.: Some aspects of ferrite cores for power transformers

CLEGG, A.G. and KEYWORTH, D.A.: Stability of rare-earth-cobalt magnets

COHEN, H.E., and GOOD, J.A.: The magnetic separation of mineral slurries by a cryogenic magnet system

COWIE, R.M., MACKINTOSH, G.H., and MESSER, P.F.: Liquid-phase sintering of barium hexaferrite magnets

DRIVER, D.R., and HANDLEY, G.W.: Nickel-iron alloys for current transformers in metering and earth-leakage protection

DRIVER, D.R., JASKO, T.M., and MAJOR, R.V.: Soft magnetic toroidal cores for r.f.i. suppression inductors

FREEMAN, E.M., and LOWTHER, D.A.: Normal force variation in single-sided linear induction machines

GOODALL, R.M.: Suspension and guidance-control system for a d.c. attraction Maglev vehicle

GRAY, P., RAYSON, H.W., and HADFIELD, D.: Early stages of decomposition of FeCrCo and Alnico permanent-magnet alloys

HILL, S., and OVERSHOTT, K.J.: The origin of the anomalous loss of grain-oriented silicon iron

HODKINSON, R.L.: 6 kW direct off-line switching power supply using ferrite transformers and inductors

HOWELL, J.P., MULHALL, B.E., and RHODES, R.G.: Electrodynamic levitation of high-speed vehicles

JAYAWANT, B.V.: Passenger-carrying vehicles using controlled d.c. and controlled permanent magnets

LINDER, D.: Design and testing of a low-speed magnetically suspended vehicle

LOWTHER, D.A., and CARPENTER, C.J.: Surface impedance characteristics of iron at 50 Hz

MAJOR, R.V., MARTIN, M.C., and BRANSON, M.W.: The development of cobalt-iron soft magnetic alloys with improved mechanical properties for use in electrical generators

MILDRUM, H.F., WONG, K.M.D., and STRNAT, K.J.: Thermal stability of rare-earth-cobalt permanent magnets

MITCHELL, R.K., and McCURRIE, R.A.: Magnetic properties of AS-cast and annealed $SmCo_{3.25}Cu_{1.75}$

MOLLARD, P., ROUSSET, A., and PARIS, J.: Physico-chemical properties of new particles of solid solutions between iron sesquioxide and divalent spinel ferrites for magnetic recording

MOSES, A.J., and PEGLER, S.M.: Effects of flexible bonding on the domain structure and magnetisation of silicon-iron laminations

OVERSHOTT, K.J., and HILL, S.: The effects of pinning on domain wall motion in 3% grain-oriented silicon-iron

POPPLEWELL, J., CHARLES, S.W., and HOON, S.R.: The long-term stability of metallic ferromagnetic liquids

RADLEY, G.S., and BANKS, P.J.: Effect of magnetostriction on Young's modulus of silicon iron subject to vibration

RILEY, P.W., and WATSON, J.H.P.: The use of paramagnetic matrices for magnetic separations

ROBINSON, A.A.: Magnetically suspended momentum wheel for satellite stabilisation

SANDERS, I.L., and COLLINS, A.J.: The effects of deposited aluminium underlays on the magnetic properties of Ni-Fe-Co films

TIMBRELL, V.: Magnetic separation of respirable asbestos fibres

WATSON, J.H.P.: Theory of high-intensity magnetic separation